ACS APPLIED MATERIALS & INTERFACES

Research Article

www.acsami.org

Nanofibers of Hydrogen-Bonded Two-Component Gel with Closely Connected p- and n-Channels and Photoinduced Electron Transfer

Pengchong Xue,* Panpan Wang, Boqi Yao, Jiabao Sun, Peng Gong, Zhenqi Zhang, Chong Qian, and Ran Lu*

State Key Laboratory of Supramolecular Structure and Materials, College of Chemistry, Jilin University, 2699# Qianjin Street, Changchun 130012, P. R. China

Supporting Information

ABSTRACT: An D−A−D gelator (DTCQ) was designed and synthesized using 2,3-dimethyl-5,8-di(thiophen-2-yl)quinoxaline and *N*-alkyl 3-aminocarbazole units as acceptor and donor, respectively, which were linked by a single bond. The compound could gelate several solvents, such as benzyl alcohol, aniline, acetophenone, and *o*-dichlorobenzene, as well as self-assemble into one-dimensional (1D) nanofibers in gel phase. The absorption and infrared spectra of the gels indicated that $\pi-\pi$ interactions between aromatic moieties, intermolecular hydrogen bonds between amide units, and van der Waals forces were the driving forces for the formation of 1D self-assemblies and gel. DTCQ gel was red and emits red fluorescence because it has a strong absorption band at 487 nm and an emissive band at 620 nm. Moreover, DTCQ and a fullerene carboxylic acid formed two-component gel, in which the two compounds developed a hydrogen bond complex and self-assembled into 1D nanofibers with closely connected p- and n-channels. The nanofibrous xerogel film can rapidly generate a photocurrent under visible-light radiation through electron transfer from the gelator to fullerene, and then, the excellent exciton separation and charge transfer to two electrodes.

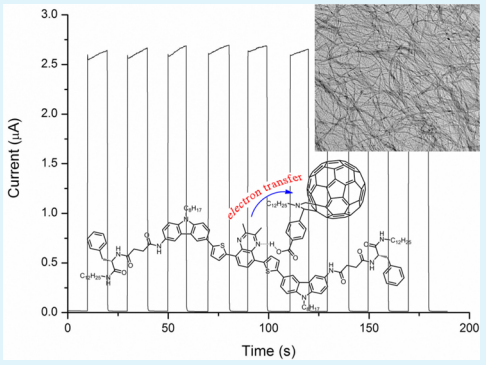

KEYWORDS: *electron transfer, photocurrent, organogels, nanofibers, fullerene, π-conjugated fluorophores*

INTRODUCTION

One-dimensional (1D) organic nanoscale self-assemblies have attracted increasing attention because of their structural flexibility, tunable optical and electrical properties, solution processability, and facile and large-scale synthesis.[1,2] They are widely used in sensors,[2−5] transistors,[6,7] batteries,[8] solar cells,[9] and nanoscale lasers[10,11] and so on. The gelation of low-molecular mass gelator in an organic solvent or water is a rapid, convenient, and low cost method to prepare 1D organic assemblies, such as nanofibers, nanoribbons, twisted nanobelts, nanorods, and nanotubes.[12−17] The morphologies and properties of these assemblies can be tuned using external chemical or physical stimuli, such as metal ions, anions, small organic compounds, proton, light irradiation, oxidation, or reduction reaction, sound, and temperature.[18−26] This tuning is achieved by introducing unique functional moieties because the driving forces for the formation of 1D self-assemblies are weak intermolecular interactions, such as hydrogen bonds, dipole−dipole interactions, $\pi-\pi$ interactions, and van der Waals forces. Moreover, the close packing between gelators in gel nanofibers is advantageous for various arrays of applications. These nanofibers have been applied in vapor sensors,[27−31] transistors,[32,33] and therapy[34,35] applications. Many two-component gels were developed to realize functionalization of gels.[36−38] In particular, the fibers in two-component gels can be used as electron donors or acceptors for photocurrent generation because of the existence of exciton diffusion. For instance, a self-sorting two-component organogel of thiophene and perylenebisimide gelators as electron donor and electron acceptors, respectively, was constructed by Shinkai et al.[39] Photocurrent is generated from the cast xerogel film upon visible-light irradiation because of the existence of p−n heterojunctions of the donor and acceptor aggregate. Würthner and Wudl applied the gel fibers as electron acceptor of decacyclene triimide and perylenebisimide gelators in a solar cell.[40,41] Stupp and Zhang synthesized tetrathiafulvalene and sexithiophene gelators, respectively, and prepared their two-component gels using fullerene as electron acceptor for photocurrent generation.[42,43]

In 2010, a hydrogen bond complex of a donor gelator and a fullerene carboxylic acid derivative serving as an electron acceptor was designed in our lab; this complex can transform into a 1D self-assembly in gel phase.[44] The donor and acceptor can be interspaced within the molecular level, and effective electron and hole transport channels exist in the fibers. Consequently, the use of these assemblies as active layers affords a large photocurrent. However, the maximal absorption peak at 357 nm is unfavorable for solar light harvesting.[45] Last

Received: September 19, 2014
Accepted: October 27, 2014
Published: October 27, 2014

year, we introduced quinoxaline as electron withdrawing group and prepared a π-conjugated gelator with a D−π−A−π−D molecular structure, which possesses a red-shifted absorption band with a maximum of 498 nm in gel.[46] The electron-donating and withdrawing groups were linked by double bonds. However, double bonds undergo topochemical [2 + 2] cycloaddition under photoirradiation.[47] So, single bonds are selected as connected type in the present study. To obtain a gelator with a long-wavelength absorption band, two thiophene units are inserted between the donor and acceptor (Scheme 1).

Scheme 1. Molecular Structures of DQTC and C12C60COOH

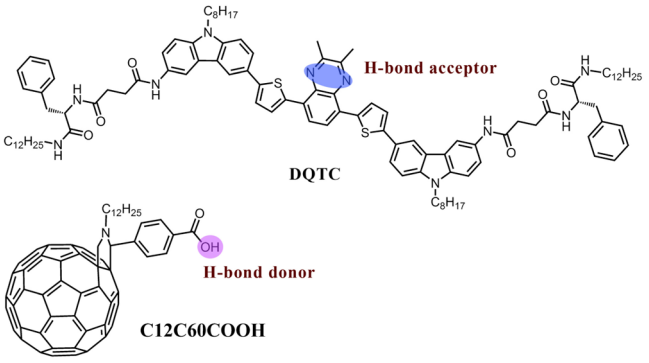

As a result, the maximum absorption peak of the gel reaches 487 nm. Moreover, a photoinduced electron transfer exists between DQTC and C12C60COOH in the two-component gel, and the xerogel film can provide a large photocurrent under visible-light irradiation.

EXPERIMENTAL SECTION

Instruments: Infrared spectra were measured using a Nicolet-360 FT-IR spectrometer by incorporating the samples in KBr disks. The UV−vis spectra were determined on a Mapada UV-1800pc spectrophotometer. C, H, and N elemental analyses were performed on a PerkinElmer 240C elemental analyzer. Mass spectra were obtained with AXIMA CFR MALDI-TOF (Compact) mass spectrometers. Photoluminescence measurements were taken on a Shimadzu RF-5301 Luminescence Spectrometer. Fluorescence decay experiment was measured on an Edinburgh FLS920 steady state fluorimeter equipped with an nF900 ns flash lamp. ^{1}H and ^{13}C NMR spectra were recorded on Mercury plus 400 MHz. Transmission electron microscopy (TEM) images were observed with a Hitachi H-8100 apparatus by wiping the samples onto a 200-mesh carbon coated copper grid followed by naturally evaporating the solvent. The fluorescence quantum yields of DQTC in THF were measured by comparing to standards (Rhodamine 6G in water, Φ_F = 0.75). Cyclic voltammetry was employed using a three-electrode cell and an electrochemistry workstation (CHI604). The working electrode was a glass carbon disc, the auxiliary electrode was a Pt wire, and Ag/AgCl was used as reference electrode. Tetrabutylammonium tetrafluoroborate ($TBABF_4$, 0.1 M) was used as the supporting electrolyte in dry DMF. The ferrocenium/ferrocene (Fc/Fc^+) redox couple was used as an internal potential reference. Geometrical optimizations for DQTC were performed by density functional theory (DFT) calculations at B3LYP/6-31G (d, p) level with the Gaussian 09W program package.[48]

Scheme 2. Synthesis Route of DQTC. (a) $Pd(PPh_3)_4$, THF; (b) NBS, THF; (c) Concentrated HNO_3, CH_2ClCH_2Cl; (d) $Pd(PPh_3)_4$, KOAc, dry DMF; (e) $Pd(PPh_3)_4$, TBAOH, THF; (f) Pd/C, NH_2NH_2, THF/ethanol; (g) dry THF; (h) EDC, DMAP, dry THF

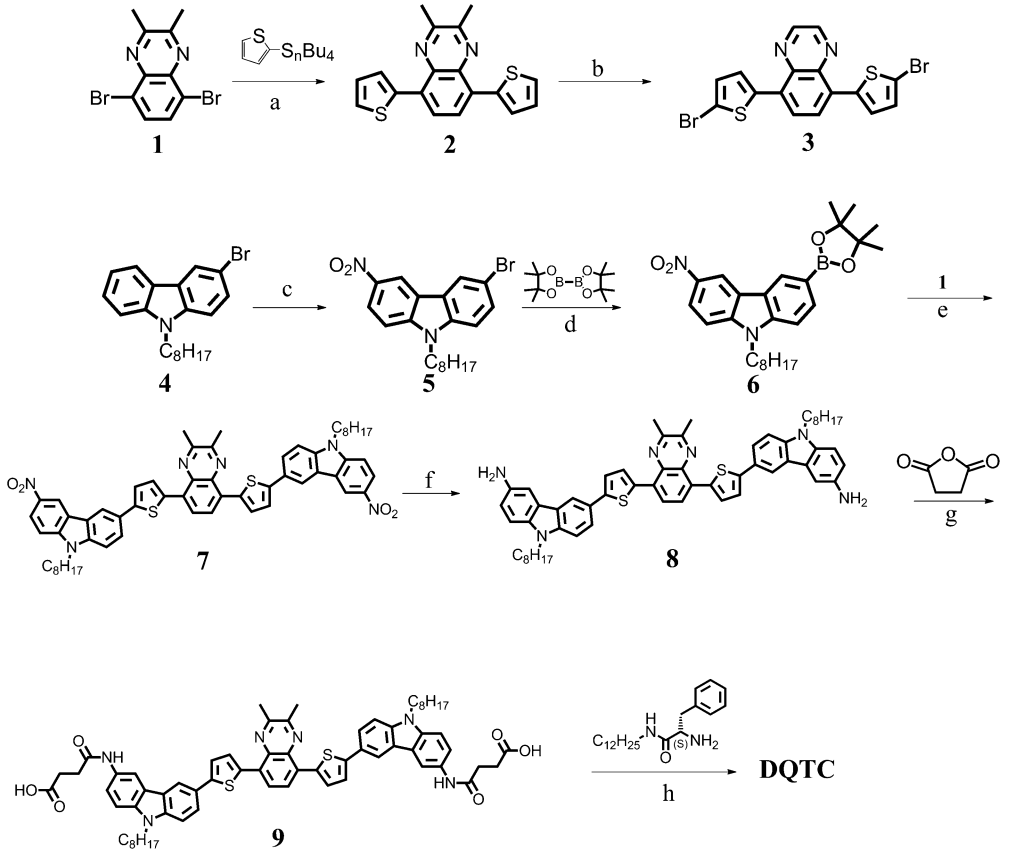

Gelation Test of Organic Fluids. The solution containing certain weighed gelator 1 in organic solvent was heated in a sealed test tube with 1 cm diameter in an oil bath until the solid was dissolved. After the solution was allowed to stand at room temperature for 6 h, the state of the mixture was evaluated by the "stable to inversion of a test tube" method.

Preparation of the ITO Active Electrode. Gelator DQTC (1.6 mg) and 1.0 mg of C12C60COOH were added to 1.6 mL *o*-dichlorobenzene and heated to complete dissolution.

This hot solution (10 μL) was quickly cast on an ITO glass electrode (electrode area 0.25 cm^2) and aged for 2 h at room temperature. The final active electrode was obtained after the solvent was removed through low pressure for 2 h and at 100 °C for 6 h. Photocurrent measurements were carried out in a nitrogen-saturated 0.1 M Na_2SO_4 solution containing 50 mM ascorbic acid (AsA) as a sacrificial electron donor using a modified ITO working electrode (0.25 cm^2) and a Pt wire counter electrode at 0 mV bias against a Ag/AgCl (3.0 M KCl) reference electrode. A collimated light beam (50 mW cm^{-2}) from a 150 W Xe lamp was used for the excitation of ITO active films.

Synthesis and Characteristics. (S)-2-amino-N-dodecyl-3-phenylpropanamide, 5,8-dibromo-2,3-dimethylquinoxaline (**1**), and 3-bromo-9-octyl-9H-carbazole were synthesized according to the lecture procedures.[49−51] The synthesis route of DQTC is shown in Scheme 2.

5,8-bis(5-bromothiophen-2-yl)-2,3-dimethylquinoxaline (3). 5,8-dibromo-2,3-dimethylquinoxaline (2.0 g, 6.33 mmol), 2-(tributylstannyl)thiophene (5.19 g, 13.9 mmol), and $Pd(PPh_3)_2Cl_2$ (200 mg) was added into 50 mL dry THF, and the mixture was refluxed for 2.5 h under N_2 atmosphere. After removing solvent, the residue was purified by silica column chromatography (CH_2Cl_2/petroleum ether, V/V = 1:1). Light yellow solid (1.7 g, 83.3%) was obtained (^{1}H NMR (400 MHz, $CDCl_3$) δ 8.04 (s, 2H), 7.85 (d, J = 3.4 Hz, 2H), 7.49 (d, J = 4.9 Hz, 2H), 7.23−7.09 (m, 2H), 2.82 (s, 6H)). The weighted yellow solid (1.3 g, 4 mmol) was dissolved into THF (80 mL), and NBS (1.4 g, 8 mmol) was added into above solution slowly. After stirring for 12 h, the mixture was poured into water (400 mL) and the solid was gained by filtration and purified by silica column chromatography (CH_2Cl_2). 1.4 g orange solid was gained. Yield = 72.3%. Elemental analysis (%): calculated for $C_{18}H_{12}Br_2N_2S_2$: C, 45.02; H, 2.52; N, 5.83; found, C, 44.98; H, 2.49; N, 5.86. FT-IR (KBr, cm^{-1}): 3167, 3078, 2956, 2923, 1613, and 1539. ^{1}H NMR (400 MHz, $CDCl_3$) δ 8.07 (s, 2 H, =CH), 7.27 (d, J = 6.2 Hz, 2 H, =CH), 7.03 (d, J = 6.2 Hz, 2 H, =CH), 2.76 (s, 6 H, CH_3). ^{13}C NMR (101 MHz, $CDCl_3$) δ 152.61, 139.83, 136.71, 130.13, 128.98, 125.26, 124.67, 116.90, 22.49.

3-Bromo-6-nitro-9-octyl-9H-carbazole (5). **4** (10.0 g, 27.9 mmol) was dissolved in 50 mL CH_2ClCH_2Cl. After the solution was stirred for 10 min at an ice−water bath, 3.0 g of concentrated HNO_3 was added dropwise over 1 h. The mixture was stirred at room temperature for 10 h and the yellow solid was obtained by filtration. The solid was purified using column chromatography (petroleum ether/CH_2Cl_2, V/V = 1:1) to give yellow product (7.1 g, 61% in yield). Elemental analysis (%): calculated for $C_{20}H_{23}BrN_2O_2$: C, 59.56; H, 5.75; N, 6.95; found C, 59.54; H, 5.71; N, 6.93. FT-IR (KBr, cm^{-1}): 3088, 2920, 2853, 1620, 1596, 1583, 1513, 1476, and 1319. ^{1}H NMR (400 MHz, $CDCl_3$) δ 9.00 (d, J = 16 Hz, 1H, =CH), 8.40 (dd, J = 8.0, 6.3 Hz, 1H, =CH), 8.27 (d, J = 4.5 Hz, 1H, =CH), 7.70 (d, J = 6.5 Hz, 1H, =CH), 7.40 (dd, J = 9.0, 4.3 Hz, 1H, =CH), 7.36 (d, J = 4.0 Hz, 1H, =CH), 4.37 (t, J = 8.5 Hz, 2H, N−CH_2), 1.88 (m, 2H, −CH_2), 1.42−1.17 (m, 10H, −CH_2), 0.86 (t, J = 6.4 Hz, 3H, −CH_3). ^{13}C NMR (101 MHz, $CDCl_3$) δ 143.64, 140.86, 140.27, 130.12, 124.48, 123.75, 122.16, 121.44, 117.53, 113.61, 111.14, 108.61, 43.79, 31.71, 29.26, 29.10, 28.87, 27.20, 22.57, 14.04.

3-Nitro-9-octyl-6-(4,4,5,5-tetramethyl-1,3,2-dioxaborolan-2-yl)-9H-carbazole (6). **5** (5.1 g, 12.16 mmol), bis(pinacolato)diboron (3.7 g, 14.57 mmol), KOAc (3.6 g, 36.7 mmol), and $Pd(PPh_3)_4$ (50 mg) were wadded in 80 mL dry DMF. The mixture was stirred under a N_2 atmosphere at 90 °C for 24 h. The mixture was poured into 500 mL water and extracted with CH_2Cl_2. The combined organic phases were washed with brine and dried with anhydrous Na_2SO_4. After solvent was removed, the residue was purified by column chromatography (petroleum ether/CH_2Cl_2, V/V = 1:1) to give a yellow solid (3.78 g) in a yield of 69%. Elemental analysis (%): calculated for $C_{26}H_{35}BN_2O_4$: C, 69.34; H, 7.83; N, 6.22; found C, 69.32; H, 7.85; N, 6.19. FT-IR (KBr, cm^{-1}): 3090, 3063, 2991, 2974, 2954, 2931, 2870, 2854, 1632, 1599, 1516, 1482, 1468, 1328, 1259, and 1142. ^{1}H NMR (400 MHz, $CDCl_3$) δ 9.10 (d, J = 8.5 Hz, 1H, =CH), 8.69 (dd, J = 8.4, 2.3 Hz, 1H, =CH), 8.41 (d, J = 6.5 Hz, 1H, =CH), 8.02 (d, J = 9.0 Hz, 1H, =CH), 7.45 (m, 2H, =CH), 4.37 (t, J = 7.4 Hz, 2H, N−CH_2), 1.90 (m, 2H, −CH_2), 1.43−1.28 (m, 10H, −CH_2), 1.25 (m, 12H, −CH_3), 0.90 (t, J = 6.3 Hz, 3H, −CH_3). ^{13}C NMR (101 MHz, $CDCl_3$) δ 143.73, 143.65, 140.97, 133.61, 128.32, 127.35, 122.85, 122.53, 121.63, 117.37, 109.04, 108.34, 83.90, 43.65, 31.73, 29.28, 29.10, 28.89, 27.20, 24.95, 22.57, 14.04.

6,6′-(5,5′-(2,3-Dimethylquinoxaline-5,8-diyl)bis(thiophene-5,2-diyl))bis(3-nitro-9-octyl-9H-carbazole) (7). **3** (0.66 g, 1.38 mmol), **6** (1.5 g, 3.33 mmol), $Pd(PPh_3)_4$ (30 mg), and TB_4NOH (6.0 g, 25% in water) was added into 50 mL THF. The mixture was heat to reflux under a N_2 atmosphere for 48 h. The mixture was cooled to room temperature and red solid was obtained by suction filtration and washed by ethanol. Red product was obtained after drying. Yield = 87%. Elemental analysis (%): calculated for $C_{58}H_{58}N_6O_4S_2$: C, 72.02; H, 6.04; N, 8.69; found C, 71.92; H, 5.99; N, 8.64. IR (KBr, cm^{-1}): 2926, 1597, 1506, 1472, and 1394. MS, *m*/*z*: cal. 967.25, found 968.40 $[M + H]^+$. Because of its low solubility, NMR spectra did not gain.

6,6′-(5,5′-(2,3-Dimethylquinoxaline-5,8-diyl)bis(thiophene-5,2-diyl))bis(9-octyl-9H-carbazol-3-amine) (8). **7** (0.55 g, 0.57 mmol) and hydrazine hydrate (0.57 g, 80%) were dissolved in 10 mL THF/ethanol (V/V = 1/1). After adding Pd/C (10 mg), the mixture was heated to reflux for 10 h. Pd/C was filtered and the red solid was obtained by removing solvent. The solid was dispersed in 10 mL CH_2Cl_2 and treated for 5 min in an ultrasound bath. The red product was given by filtration and drying. Yield = 62%. Elemental analysis (%): calculated for $C_{58}H_{62}N_6S_2$: C, 76.78; H, 6.89; N, 9.26; found C, 76.72; H, 6.83; N, 9.23. FT-IR (KBr, cm^{-1}): 3371, 3208, 3069, 2950, 2925, 2853, 1632, 1608, 1537, 1485, and 950. ^{1}H NMR (400 MHz, DMSO) δ 8.33 (d, J = 1.3 Hz, 2H), 8.25 (s, 2H), 8.01 (d, J = 3.9 Hz, 2H), 7.76 (dd, J = 8.5, 1.4 Hz, 2H), 7.55 (d, J = 3.9 Hz, 2H), 7.52 (d, J = 8.7 Hz, 2H), 7.40 (d, J = 1.9 Hz, 2H), 7.32 (d, J = 8.7 Hz, 2H), 6.87 (dd, J = 8.6, 2.0 Hz, 2H), 4.82 (b, 4H), 4.29 (t, J = 6.6 Hz, 4H), 2.88 (s, 6H), 1.74 (m, 4H), 1.31−1.10 (m, 20H), 0.82 (t, J = 6.8 Hz, 6H). ^{13}C NMR (101 MHz, d_6-DMSO) δ 152.94, 148.20, 141.95, 140.11, 136.55, 136.04, 134.02, 129.88, 128.01, 125.35, 124.27, 123.33, 122.90, 122.45, 121.86, 116.91, 115.86, 110.02, 109.65, 104.49, 31.34, 28.92, 28.78, 26.66, 25.07, 22.67, 22.19, 14.08.

4,4′-((6,6′-(5,5′-(2,3-Dimethylquinoxaline-5,8-diyl)bis(thiophene-5,2-diyl))bis(9-o ctyl-9H-carbazole-6,3-diyl))bis(azanediyl))bis(4-oxobutanoic acid) (9). **8** (0.6 g, 0.66 mmol) and succinic anhydride (0.14 g, 1.4 mmol) was dissolved in 10 mL dry THF and stirred for 10 h. After removing solvent, the residue was dispersed in methanol and treated for 5 min by ultrasonic. The red product was gained by filtration. Yield = 65%. Elemental analysis (%): calculated for $C_{66}H_{70}N_6O_6S_2$: C, 71.58; H, 6.37; N, 7.59; found C, 71.52; H, 6.39; N, 7.53. IR (KBr, cm^{-1}): 3130, 2920, 1714, 1592, and 1398. MS, *m*/*z*: cal. 1106.5, found 1107.5 $[M + H]^+$. Because of its low solubility, NMR spectra did not gain.

N^1,$N^{1\prime}$-(6,6′-(5,5′-(2,3-dimethylquinoxaline-5,8-diyl)bis(thiophene-5,2-diyl))bis(9-octyl-9H-carbazole-6,3-diyl))bis(N4-(1-(dodecylamino)-1-oxo-3-phenylpropan-2-yl)succinamide) (DQTC). To the mixture of **9** (0.20 g, 0.18 mmol), (S)-2-amino-N-dodecyl-3-phenylpropanamide (0.176 g, 0.53 mmol), and DMAP (10 mg) was added dry THF (20 mL). After the mixture was stirred in an ice−water bath for 10 min, EDC·HCl (0.10 g) was added. The mixture was warmed slowing to room temperature and stirred 10 h. Ethanol (50 mL) was added, and then, the red solid was obtained by suction filtration and washed by ethanol few times. Yield: 95%. Elemental analysis (%): calculated for $C_{108}H_{138}N_{10}O_6S_2$: C, 74.70; H, 8.01; N, 8.07; found C, 74.66; H, 7.98; N, 8.11. ^{1}H NMR (400 MHz, d_6-DMSO) δ10.06 (s, 2H), 8.58 (s, 2H), 8.40 (s, 2H), 8.30 (m, 4H), 8.06 (d, J = 3.2 Hz, 2H), 7.87 (m, 4 H), 7.66 (d, J = 8.6 Hz, 2 H), 7.61 (d, J

= 3.2 Hz, 2H), 7.60−7.47 (m, 4H), 7.35−7.1 (m, 10H), 4.40 (m, 6 H), 3.12−3.07 (m, 6 H), 2.90 (s, 6H), 2.78 (dd, J = 8.5, 6.4 Hz, 2 H), 2.71−2.56 (m, 8H), 1.83 (m, 4H), 1.41−0.90 (m, 60H, CH_2), 0.90−0.71 (m, 12H, CH_3). MS, *m*/*z*: cal. 1736.0, found 1736.4 $[M]^+$.

RESULTS AND DISCUSSION

Molecular Design and Synthesis. Considering that sp^2 hybridized N atoms are good hydrogen bond acceptors,[52] quinoxaline was introduced. 3-Aminocarbazole can serve as a donor moiety. If quinoxaline and carbazole are directly connected using double bond from a heck reaction, a red solid with a maximum absorption around 487 nm can be obtained.[46] The compound will possess a blueshifted absorption band if the two moieties are linked by a single bond. Thiophene is a suitable group to regulate the molecular energy levels and absorption spectra of the materials.[53,54] Therefore, two thiophene units were selected to link the carbazole and quinoxaline moieties to provide a chromophore with the ability to absorb long-wavelength light. Chiral amine acid moieties with long alkyl chains were linked with fluorophores to ensure that whole molecules can self-assemble into 1D nanostructures.[55] Scheme 2 shows the detailed synthesis route. Compound **3** was synthesized from 5,8-dibromo-2,3-dimethylquinoxaline through a Stille reaction with 2-(tributylstannyl)thiophene followed by bromination. **4** was nitrated with concentrated HNO_3 to obtain **5**. The reaction of **5** and bis(pinacolato)diboron yielded **6**, which was coupled with **3** to produce **7** via a Suzuki reaction. Compound **8** was easily obtained with a high yield from **7** using NH_2NH_2 as a reducing agent. The rapid amidation of compound **8** with succinic anhydride generated a carboxylic acid derivative (**9**). The condensation reaction of (S)-2-amino-N-dodecyl-3-phenylpropanamide and compound **9** in the presence of EDC·HCl was utilized to obtain DQTC.

Photophysical Properties in Solution. DQTC can be dissolved in THF to obtain a red solution. The maximum absorption peak at long-wavelength region is located at 483 nm (Figure 1a) and has a high absorption coefficient (5.2×10^4 M^{-1} cm^{-1}), which is adequately significant for the compound to absorb sunlight.[56] Moreover, the red THF solution emits strong red fluorescence under 365 nm irradiation. The emission band shows a maximum at 605 nm. The fluorescence quantum is moderate and reaches 0.32, which indicates that DQTC is a better red fluorescent dye. The fluorescence decay of DQTC in THF is single exponential decay process, and the lifetime (τ) is 4.4 ns. Radiative (K_r) and nonradiative (K_{nr}) rate constants are 0.072 and 0.14 ns^{-1} (Supporting Information Figure S1), which explain the moderate fluorescence quantum. When dissolved in DMF and DMSO, the absorption shows slight spectral redshifts (<2 nm), whereas the DMF and DMSO solutions exhibit evident red-shifted fluorescence bands relative to those of THF (Figure 1b). These results suggest that DQTC has an excited state with larger dipole moment than that in the ground state.[57] Considering the D−A−D molecular structure of the chromophore; the red-shifted fluorescence in large polar solvents can be attributed to the intramolecular charge transition after visible-light excitation. The results of the quantum chemical calculation can support this explanation. Figure 1c shows that the HOMO state density was completely distributed over the linearly conjugated moiety, and the pyrazine ring has a significantly low density. In contrast, the electron density of LUMO was mainly localized in the quinoxaline and two thiophene moieties. Thus, when DQTC

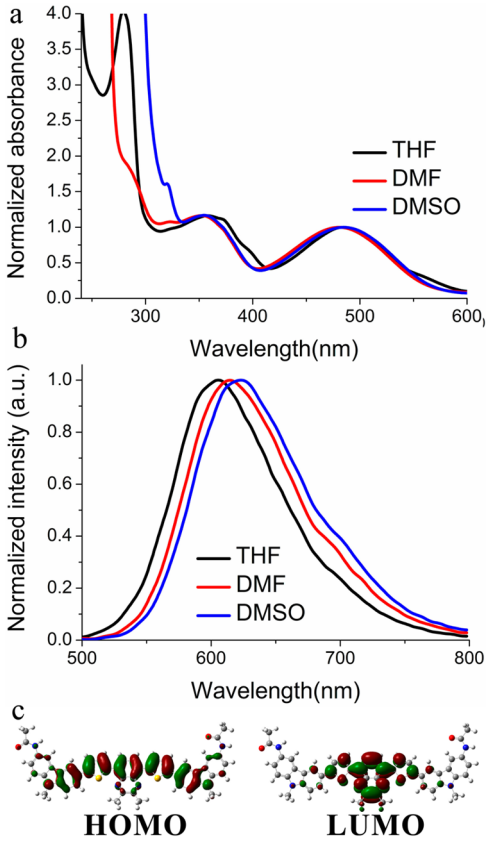

Figure 1. (a) Absorption and (b) fluorescence of DQTC in different solvents and (c) orbital distribution of LUMO and HOMO for DQTC. To simplify the calculation, only the chromophore was selected and the long alkyl chain was replaced with methyl group.

is excited by visible light, accompanied by an intramolecular charge transfer, an excited state with larger polarity can be observed. At this time, the electron in LUMO is mainly located at the acceptor, which is beneficial for the electron transfer from DQTC to fullerene after visible-light excitation because fullerene is near the quinoxaline moiety in the complex (see below).

A basic premise for realizing a photoinduced electron from the excited DQTC to fullerene is that the electron donor should have a sufficiently high LUMO relative to one of the fullerene. Thus, electrochemical properties were determined through cyclic voltammetry. The HOMO energy level (−4.80 eV) of DQTC was estimated from the first oxidation potential using the ferrocenium/ferrocene (Fc/Fc^+) redox couple as an internal potential reference. The LUMO energy level of DQTC can be evaluated using the following equation: $E_{LUMO} = E_{HOMO} + E_{0-0}$, where E_{0-0} is the 0−0 excitation energy and is 2.15 eV as obtained from the edge of the absorption spectrum in THF. The E_{LUMO} value (−2.77 eV) is determined, which is sufficiently high relative to the LUMO energy level (−3.66 eV) of C12C60COOH. Based on these optical and electrochemical observations, DQTC is, therefore, an excellent electron donor and light-harvesting antenna.

Self-Assembly of DQTC in Gel Phase. First, the gelation ability of DQTC was investigated through the standard heating-and-cooling method (Table 1). DQTC (1.0 mg) was dissolved in 1.0 mL of DMF, DMSO, or THF with heating. After cooling to room temperature, the DMF and DMSO solutions remained clear, whereas red deposition was observed in THF. The

Table 1. Gelation Ability of DQTC in Organic Solvents[a]

solvents	DQTC	solvents	DQTC
DMF	S	toluene	I
DMSO	S	*o*-dichlorobenzene	G (2.0)[b]
THF	P	acetophenone	G (3.3)[b]
CH_2Cl_2	I	aniline	G (2.2)[b]
hexane	I	benzyl alcohol	G (3.3)
cyclohexane	I	ethanol	I
benzene	I	ethyl acetate	I

[a]Gelator = 1.0 mg/mL; G, gel; I, insoluble; P, precipitate. [b]Critical gelation concentration (mg/mL).

compound has significantly low solubility in hexane, cyclohexane, benzene, toluene, ethanol, and ethyl acetate, even with heating. Fortunately, the hot red solutions in polar aromatic solvents, such as *o*-dichlorobenzene (ODCB), acetophenone, and aniline, can be converted into red gels when cooled to room temperature. DQTC also gelates with benzyl alcohol to form a red gel. The results suggest that DQTC can form gels in polar aromatic solvents. Moreover, DQTC has a small critical gelation concentration in these solvents. For instance, 2 mg of DQTC can prevent the flowing of 1 mL of ODCB and aniline. Thus, one DQTC molecule can gelate more than 15400 ODCB and 19000 aniline molecules.

When the gelation ability of DQTC was measured, the hot sol and gel had different colors and emissive colors (Figure 2c), which are indicative of the existence of $\pi-\pi$ interactions in the gel phase.[58,59] Therefore, the absorption and fluorescence spectra were used to monitor the gelation process. Figure 2 shows that the orange hot sol at 120 °C has a maximum absorption peak at 469 nm, which gradually redshifts and increases in absorbance. After cooling to room temperature, a dark red gel is formed, which possesses a red-shifted absorption peak at 488 nm, indicating a shift of 19 nm. This spectral shift shows that $\pi-\pi$ interactions exist between the aromatic moieties and stack together in a head-to-tail model (*J*-aggregate),[60,61] which provides exciton transfer channel. A fluorescence spectral change was also used to observe the intermolecular interaction. The hot ODCB sol of DQTC at 120 °C has a strong and wide emission peak at 600 nm, which gradually redshifts and weakens in emission intensity. The gel at room temperature emits red fluorescence with a maximum value at 624 nm, which also indicates $\pi-\pi$ interactions between the gelators. The circular dichroism (CD) spectrum also supports the $\pi-\pi$ interaction because two weak peaks at 342 and 518 nm were observed in the gel phase (Supporting Information Figure S2). The weak signals in the CD spectrum indicate low twisted angle between two adjacent DQTC molecules.[62]

Hydrogen bonds are the main driving forces for the self-assembly of a gelator in organic solvents. The Fourier transform infrared (FT-IR) spectrum of the xerogel film was obtained. The results of extensive studies imply that the secondary amino groups (NH) in the amide moiety involved in the amide–amide hydrogen bonds (C═O···H—N) display stretching bands within 3370–3250 cm^{-1}. The bands located within 3500–3400 cm^{-1} can be generally ascribed to the amide groups that are not involved in hydrogen bonds.[63] The FT-IR spectrum of DQTC in the ODCB gel exhibited an absorption band at 3287 cm^{-1} (Supporting Information Figure S3), indicating that all N–H groups are involved in hydrogen bonds. The Amide I bands ascribed to the aromatic and aliphatic

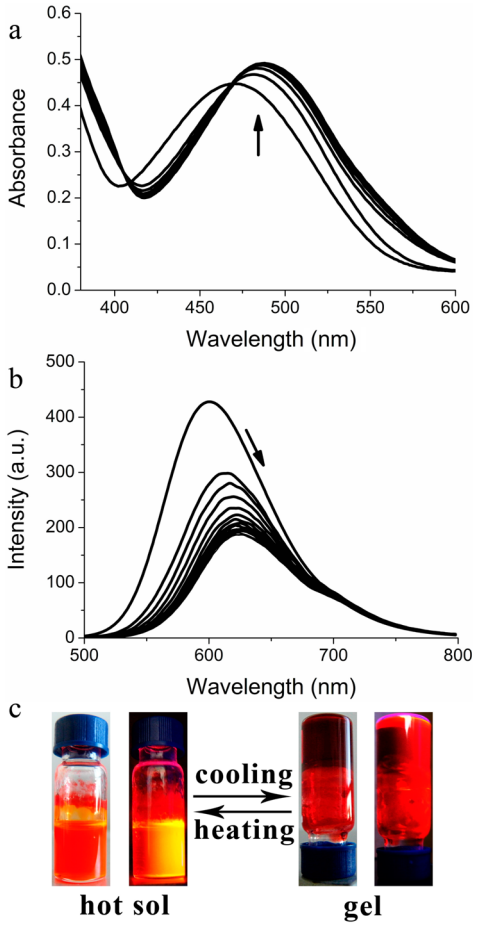

Figure 2. (a) Absorption and (b) fluorescence spectral changes of DQTC in ODCB from hot sol to gel (120 to 20 °C, interval is 5 °C). (c) Photos of DQTC under natural light (left) and 365 nm light (right). Concentration is 2.0 mg/mL.

amide moieties appeared at 1652 and 1637 cm^{-1}, respectively. This result indicates that all amide groups are involved in intermolecular hydrogen bonds.[64−67] The FT-IR analyses also provide information on alkyl chains. The absorption bands of the antisymmetric (ν_{as}) and symmetric (ν_{as}) CH_2 stretching vibrations of DQTC appeared at 2921 and 2852 cm^{-1}, respectively, indicating a close stacking between alkyl chains.[68] These spectral observations evidently support the theory that hydrogen bonds, van der Waals forces, and $\pi-\pi$ interactions are the driving forces of gel formation.

To gain direct insight into the nature of the self-assembled microstructures, transmission electron microscopy (TEM) was used. The TEM image of the dried gel revealed that DQTC self-assembled into 1-D nanofibers as shown in Figure 3a. The diameters of the thin fibers range from 40 to 100 nm. Several thin fibers stack together to form a wide fiber. Therefore, the gelation procedure can be described. As shown in Figure 4, the gelators exist as monomers in the hot sol and begin to form small 1D aggregates inducing by weak intermolecular interactions when the temperature decreases. These small aggregates further grow into 1D nanofibers, which twine around each other to form wide fibrous bundles. Finally, thin and wide fibers generate an extended 3D fibrillar network that stabilizes the gel state. Moreover, the molecular stacking in the 1D direction provides an efficient carrier pathway along the fibrous direction.

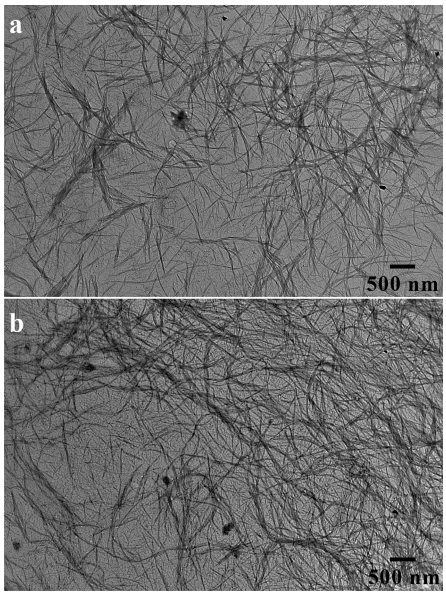

Figure 3. TEM images of (a) xerogel and (b) two-component xerogel (molar ratio = 1:1).

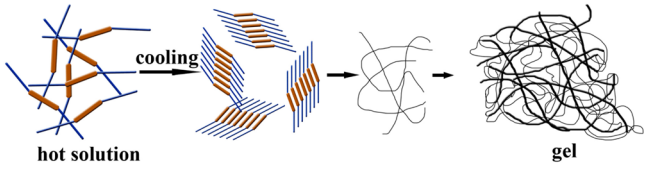

Figure 4. Schematic of molecular self-assembly of DQTC during gelation.

Two-Component Gel of DQTC and C12C60COOH. As discussed above, DQTC has a proper LUMO energy level that promotes electron transfer from the excited DQTC to the fullerene derivative after visible-light excitation, accompanied by the fluorescence quenching of DQTC as an electron donor if the two compounds are close. Thus, the fluorescence spectra were obtained after adding C12C60COOH to the DQTC gel. The addition of C12C60COOH did not destroy the gel phase of DQTC, and thus, two-component gels appeared. However, the fluorescence intensities of these two-component gels are relative to the amount of the electron acceptor (Figure 5a). A higher amount of C12C60COOH results in a weaker fluorescence. This fluorescence quenching can be ascribed to the electron transfer.[69] The fluorescence lifetime measurements also imply an electron transfer process from DQTC to C60 derivative. The average fluorescence lifetime ($\langle\tau\rangle$) of DQTC gel is 6.22 ns. It decreases to 5.1 ns in two-component gel (molar ratio = 1:1, Supporting Information Figure S1), ascribing to the existence of photoinduced electron transfer. Adding of C12C60COOH could affect the stability of gels. For example, T_{gel} of neat gel at a concentration of 1.6 mg/mL is 60 °C, which increases to 65 °C for two-component gel at the same concentration of DQTC. Moreover, the two-component gels maintained their red color, and their absorption bands were a simple overlapping of the bands of C12C60COOH and aggregated DQTC (Figure 5b). The two-component gel has similar CD spectrum to that of neat DQTC, except for the enhanced signal intensity, which may be caused by the increase in the twisted angle between two adjacent DQTCs. The vibration absorption peaks ascribed to the amide groups in IR

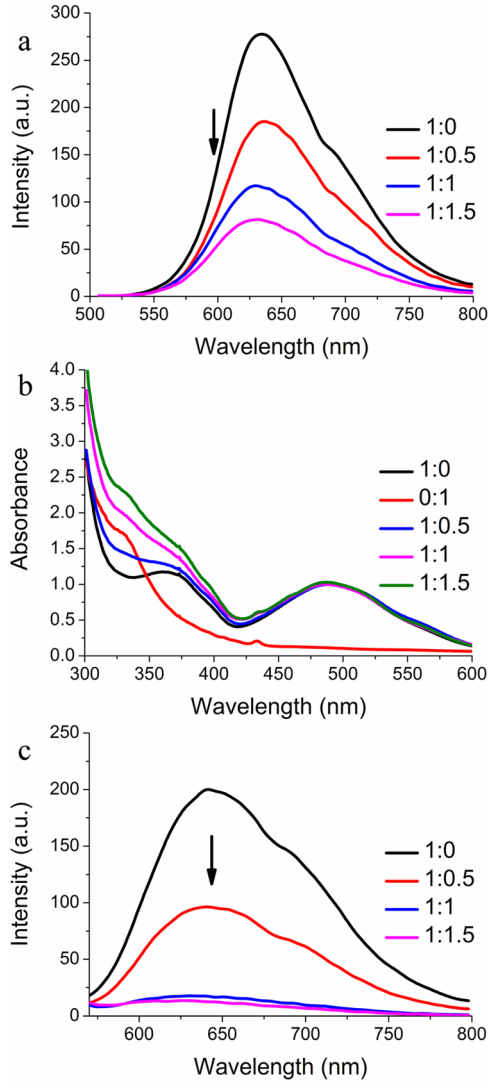

Figure 5. Emission (a for wet gel; c for gel film) and absorption spectra (b) of two component gels with different molar ratio. λ_{ex} = 489 nm.

spectra of the two-component gel are identical to those of the neat DQTC. Moreover, the vibration peak of C12C60COOH at 1692 cm^{-1} ascribed to the carboxylic dimer was observed until the molar ratio of C12C60COOH and DQTC was greater than 1 (Supporting Information Figure S4). This result implies that C12C60COOH and DQTC formed a hydrogen-bonding complex with a 1:1 stoichiometry in the gel phase. The TEM image of the two-component gel (1:1) is similar to that of the neat gel, and no large C12C60COOH aggregates are found (Figure 3b). These spectral results suggest that the stacking model of DQTC did not change, and the 1D carrier transporting channel of DTQC was maintained after linking with C12C60COOH through hydrogen bonding. In addition, the fluorescence of the wet gel was not completely quenched, even when 1.5-equiv electron acceptor was added. The residual emission of the two-component wet gel could originate from the gelator molecules in the solution state because the fluorescence is completely quenched in the two-component xerogel (1:1) film.

As previously shown, electron transfer was noted from DQTC to C12C60COOH, a 1D aggregate of DQTC remains,

dx.doi.org/10.1021/am506422m | ACS Appl. Mater. Interfaces 2014, 6, 21426−21434

and the order arrangement of C12C60COOH induced by DQTC aggregates also exist. Therefore, the two-component xerogel fibrous film may serve as an active layer to generate a photocurrent. The photocurrent measurements for the indium tin oxide (ITO) electrodes coated with two-component xerogel films (as the working electrode) were performed using ascorbic acid as a sacrificial electron donor, a platinum wire as a counter electrode, and Ag/AgCl as a reference electrode.[70] Figure 6

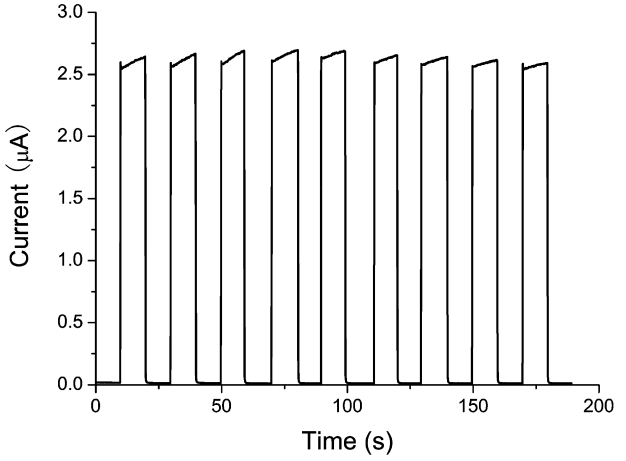

Figure 6. Photocurrent response of ITO electrodes with two-component xerogel (1:1) films; applied potential is 0 V vs Ag/AgCl.

shows that the current is significantly low (1.7×10^{-2} μA) when the electrode is placed in the dark. Stable photocurrents immediately appear upon visible-light irradiation and increase for more than 100 times relative to that in the dark. The photocurrent can instantly decrease to its initial value when the illumination is removed. The response is reversibly repeated several times, indicating that the xerogel film is sufficiently stable. The result proves that such xerogel film is undoubtedly an excellent candidate for photocurrent generation because an electron transfer occurs from the gelator to fullerene, as well as an excellent exciton separation and electron transfer to the two electrodes.

CONCLUSION

2,3-Dimethyl-5,8-di(thiophen-2-yl)quinoxaline and *N*-alkyl 3-aminocarbazole units, which serve as electron acceptor and donor, respectively, and are linked by a single bond, are used to prepare a D−A−D gelator. Target compound can gelate several solvents and self-assemble into 1D nanofibers in gel phase. The absorption and IR spectra of the gels indicate that the $\pi-\pi$ interactions between the aromatic moieties, intermolecular hydrogen bonds between amide units and van der Waals force are the driving forces for the formation of the 1D self-assemblies and gel. The gel has a strong absorption band at 487 nm, implying an improved light-harvesting antenna. Moreover, the gelator and a fullerene carboxylic acid generated a hydrogen bond complex and self-assembled into 1D nanofibers with closely connected p- and n-channels in the two-component gels. The nanofibrous xerogel film can rapidly generate a photocurrent under visible-light radiation because of electron transfer from the gelator to fullerene. Further studies are needed to provide a gelator donor with absorption within the long-wavelength region.

ASSOCIATED CONTENT

Supporting Information

NMR spectrum and MS of DQTC; CD and FT-IR spectra of neat and two component gels; time-resolved fluorescence spectra of DQTC in THF solution, ODCB gel, and two-component gel. This material is available free of charge via the Internet at http://pubs.acs.org.

AUTHOR INFORMATION

Corresponding Authors

*E-mail: xuepengchong@jlu.edu.cn.
*E-mail: luran@mail.jlu.edu.cn.

Author Contributions

The manuscript was written through contributions of all authors. All authors have given approval to the final version of the manuscript.

Notes

The authors declare no competing financial interest.

ACKNOWLEDGMENTS

This work was financially supported by the National Natural Science Foundation of China (21103067 and 21374041), the Youth Science Foundation of Jilin Province (20130522134JH), the Open Project of the State Key Laboratory of Supramolecular Structure and Materials (SKLSSM201407), the Open Project of State Laboratory of Theoretical and Computational Chemistry (K2013-02).

REFERENCES

(1) Zhang, C.; Yan, Y.; Zhao, Y. S.; Yao, J. Synthesis and Applications of Organic Nanorods, Nanowires, and Nanotubes. *Annu. Rep. Prog. Chem., Sect. C: Phys. Chem.* **2013**, *109*, 211−239.
(2) Park, C.; Park, J. E.; Choi, H. C. Crystallization-Induced Properties from Morphology-Controlled Organic Crystals. *Acc. Chem. Res.* **2014**, *47*, 2353−2364.
(3) Wang, X.; Drew, C.; Lee, S.-H.; Senecal, K. J.; Kumar, J.; Samuelson, L. A. Electrospun Nanofibrous Membranes for Highly Sensitive Optical Sensors. *Nano Lett.* **2002**, *2*, 1273−1275.
(4) Chen, X.; Wong, C. K.Y.; Yuan, C. A.; Zhang, G. Nanowire-Based Gas Sensors. *Sens. Actuators, B* **2013**, *177*, 178−195.
(5) Zhao, Y. S.; Wu, J.; Huang, J. Vertical Organic Nanowire Arrays: Controlled Synthesis and Chemical Sensors. *J. Am. Chem. Soc.* **2009**, *131*, 3158−3159.
(6) Park, K. S.; Cho, B.; Baek, J.; Hwang, J. K.; Lee, H.; Sung, M. M. Single-Crystal Organic Nanowire Electronics by Direct Printing from Molecular Solutions. *Adv. Funct. Mater.* **2013**, *23*, 4776−4784.
(7) Tucker, N. M.; Briseno, A. L.; Acton, O.; Yip, H.; Ma, H.; Jenekhe, S. A.; Xia, Y.; Jen, A. K. Y. Solvent-Dispersed Benzothiadiazole-Tetrathiafulvalene Single-Crystal Nanowires and Their Application in Field-Effect Transistors. *ACS Appl. Mater. Interfaces* **2013**, *5*, 2320−2324.
(8) Luo, C.; Huang, R.; Kevorkyants, R.; Pavanello, M.; He, H.; Wang, C. Self-Assembled Organic Nanowires for High Power Density Lithium Ion Batteries. *Nano Lett.* **2014**, *14*, 1596−1602.
(9) Hirade, M.; Nakanotani, H.; Yahiro, M.; Adachi, C. Formation of Organic Crystalline Nanopillar Arrays and Their Application to Organic Photovoltaic Cells. *ACS Appl. Mater. Interfaces* **2011**, *3*, 80−83.
(10) Liao, Q.; Xu, Z.; Zhong, X.; Dang, W.; Shi, Q.; Zhang, C.; Weng, Y.; Lid, Z.; Fu, H. An Organic Nanowire Waveguide Exciton−Polariton Sub-Microlaser and Its Photonic Application. *J. Mater. Chem. C* **2014**, *2*, 2773−2778.
(11) Guo, P.; Zhuang, X.; Xu, J.; Zhang, Q.; Hu, W.; Zhu, X.; Wang, X.; Wan, Q.; He, P.; Zhou, H.; Pan, A. Low-Threshold Nanowire Laser

Based on Composition-Symmetric Semiconductor Nanowires. *Nano Lett.* **2013**, *13*, 1251−1256.
(12) Babu, S. S.; Praveen, V. K.; Ajayaghosh, A. Functional π-Gelators and Their Applications. *Chem. Rev.* **2014**, *114*, 1973−2129.
(13) Yan, N.; Xu, Z.; Diehn, K. K.; Raghavan, S. R.; Fang, Y.; Weiss, R. G. How Do Liquid Mixtures Solubilize Insoluble Gelators? Self-Assembly Properties of Pyrenyl-Linker-Glucono Gelators in Tetrahydrofuran−Water Mixtures. *J. Am. Chem. Soc.* **2013**, *135*, 8989−8999.
(14) Babu, S. S.; Prasanthkumar, S.; Ajayaghosh, A. Self-Assembled Gelators for Organic Electronics. *Angew. Chem., Int. Ed.* **2012**, *51*, 1766−1776.
(15) Zhao, Z.; Lam, J. W. Y.; Tang, B. Z. Self-assembly of Organic Luminophores with Gelation-Enhanced Emission Characteristics. *Soft Matter* **2013**, *9*, 4564−4579.
(16) Samanta, S. K.; Bhattacharya, S. Excellent Chirality Transcription in Two-Component Photochromic Organogels Assembled through J-Aggregation. *Chem. Commun.* **2013**, *49*, 1425−1427.
(17) Babu, S. S.; Kartha, K. K.; Ajayaghosh, A. Excited State Processes in Linear π-System-Based Organogels. *J. Phys. Chem. Lett.* **2010**, *1*, 3413−3424.
(18) Wang, X.; Duan, P.; Liu, M. Universal Chiral Twist via Metal Ion Induction in the Organogel of Terephthalic Acid Substituted Amphiphilic L-Glutamide. *Chem. Commun.* **2012**, *48*, 7501−7503.
(19) Xue, P.; Sun, J.; Xu, Q.; Lu, R.; Takafuji, M.; Ihara, H. Anion Response of Organogels: Dependence on Intermolecular Interactions between Gelators. *Org. Biomol. Chem.* **2013**, *11*, 1840−1847.
(20) Ghosh, K.; Kar, D.; Panja, S.; Bhattacharya, S. Ion Conducting Cholesterol Appended Pyridinium Bisamide-Based Gel for The Selective Detection of Ag^+ and Cl^- Ions. *RSC Adv.* **2014**, *4*, 3798−3803.
(21) Qing, G.; Shan, X.; Chen, W.; Lv, Z.; Xiong, P.; Sun, T. Solvent-Driven Chiral-Interaction Reversion for Organogel Formation. *Angew. Chem., Int. Ed.* **2014**, *53*, 2124−2129.
(22) Cao, X.; Gao, A.; Lv, H.; Wu, Y.; Wang, X.; Fan, Y. Light and Acid Dual-Responsive Organogel Formation Based on *m*-Methyl Red Derivative. *Org. Biomol. Chem.* **2013**, *11*, 7931−7937.
(23) Yu, X.; Chen, L.; Zhang, M.; Yi, T. Low-Molecular-Mass Gels Responding to Ultrasound and Mechanical Stress: Towards Self-healing Materials. *Chem. Soc. Rev.* **2014**, *43*, 5346−5371.
(24) Liu, K.; Steed, J. W. Triggered Formation of Thixotropic Hydrogels by Balancing Competitive Supramolecular Synthons. *Soft Matter* **2013**, *9*, 11699−11705.
(25) Li, Y.; Lam, E. S.; Tam, A. Y.; Wong, K. M.; Lam, W. H.; Wu, L.; Yam, V. W. Cholesterol-/Estradiol-Appended Alkynylplatinum(II) Complexes as Supramolecular Gelators: Synthesis, Characterization, Photophysical, and Gelation Studies. *Chem.—Eur. J.* **2013**, *19*, 9987−9994.
(26) Dey, N.; Samanta, S. K.; Bhattacharya, S. Selective and Efficient Detection of Nitro-Aromatic Explosives in Multiple Media including Water, Micelles, Organogel, and Solid Support. *ACS Appl. Mater. Interfaces* **2013**, *5*, 8394−8400.
(27) Xue, P.; Xu, Q.; Gong, P.; Qian, C.; Ren, A.; Zhang, Y.; Lu, R. Fibrous Film of a Two-Component Organogel as a Sensor to Detect and Discriminate Organic Amines. *Chem. Commun.* **2013**, *49*, 5838−5840.
(28) Peng, H.; Ding, L.; Liu, T.; Chen, X.; Li, L.; Yin, S.; Fang, Y. An Ultrasensitive Fluorescent Sensing Nanofilm for Organic Amines Based on Cholesterol-Modified Perylene Bisimide. *Chem.—Asian J.* **2012**, *7*, 1576−1582.
(29) Zhang, X.; Liu, X.; Lu, R.; Zhang, H.; Gong, P. Fast Detection of Organic Amine Vapors Based on Fluorescent Nanofibrils Fabricated from Triphenylamine Functionalized β-Diketone-Boron Difluoride. *J. Mater. Chem.* **2012**, *22*, 1167−1172.
(30) Kartha, K. K.; Babu, S. S.; Srinivasan, S.; Ajayaghosh, A. Attogram Sensing of Trinitrotoluene with a Self-Assembled Molecular Gelator. *J. Am. Chem. Soc.* **2012**, *134*, 4834−4841.
(31) Sarkar, S.; Dutta, S.; Chakrabarti, S.; Bairi, P.; Pal, T. Redox-Switchable Copper(I) Metallogel: A Metal−Organic Material for Selective and Naked-Eye Sensing of Picric Acid. *ACS Appl. Mater. Interfaces* **2014**, *6*, 6308−6316.
(32) Hong, J. P.; Um, M. C.; Nam, S. R.; Hong, J. I.; Lee, S. Organic Single-Nanofiber Transistors from Organogels. *Chem. Commun.* **2009**, 310−312.
(33) Marty, R.; Nigon, R.; Leite, D.; Frauenrath, H. Two-Fold Odd−Even Effect in Self-Assembled Nanowires from Oligopeptide-Polymer-Substituted Perylene Bisimides. *J. Am. Chem. Soc.* **2014**, *136*, 3919−3927.
(34) Tian, R.; Chen, J.; Niu, R. The Development of Low-molecular Weight Hydrogels for Applications in Cancer Therapy. *Nanoscale* **2014**, *6*, 3474−3482.
(35) Li, P.; Dou, X.; Feng, C.; Zhang, D. Mechanical Reinforcement of C2-Phenyl-Derived Hydrogels for Controlled Cell Adhesion. *Soft Matter* **2013**, *9*, 3750−3757.
(36) Duan, P.; Cao, H.; Zhang, L.; Liu, M. Gelation Induced Supramolecular Chirality: Chirality Transfer, Amplification, and Application. *Soft Matter* **2014**, *10*, 5428−5448.
(37) Yu, X.; Cao, X.; Chen, L.; Lan, H.; Liu, B.; Yi, T. Thixotropic and Self-healing Triggered Reversible Rheology Switching in a Peptide-Based Organogel with a Cross-Linked Nano-Ring Pattern. *Soft Matter* **2012**, *8*, 3329−3334.
(38) Meazza, L.; Foster, J. A.; Fucke, K.; Metrangolo, P.; Resnati, G.; Steed, J. W. Halogen-Bonding-Triggered Supramolecular Gel Formation. *Nat. Chem.* **2013**, *5*, 42−47.
(39) Sugiyasu, K.; Kawano, S.; Fujita, N.; Shinkai, S. Self-Sorting Organogels with p−n Heterojunction Points. *Chem. Mater.* **2008**, *20*, 2863.
(40) Wicklein, A.; Ghosh, S.; Sommer, M.; Würthner, F.; Thelakkat, M. Self-Assembly of Semiconductor Organogelator Nanowires for Photoinduced Charge Separation. *ACS Nano* **2009**, *3*, 1107−1114.
(41) Pho, T. V.; Toma, F. M.; Chabinyc, M. L.; Wudl, F. Self-Assembling Decacyclene Triimides Prepared through a Regioselective Hextuple Friedel−Crafts Carbamylation. *Angew. Chem., Int. Ed.* **2013**, *52*, 1446−1451.
(42) Yang, X.; Zhang, G.; Zhang, D.; Zhu, D. A New ex-TTF-Based Organogelator: Formation of Organogels and Tuning with Fullerene. *Langmuir* **2010**, *26*, 11720−11725.
(43) Tevis, I. D.; Tsai, W.; Palmer, L. C.; Aytun, T.; Stupp, S. I. Grooved Nanowires from Self-Assembling Hairpin Molecules for Solar Cells. *ACS Nano* **2012**, *6*, 2032−2040.
(44) Xue, P.; Lu, R.; Zhao, L.; Xu, D.; Zhang, X.; Li, K.; Song, Z.; Yang, X.; Takafuji, M.; Ihara, H. Hybrid Self-Assembly of a π Gelator and Fullerene Derivative with Photoinduced Electron Transfer for Photocurrent Generation. *Langmuir* **2010**, *26*, 6669−6675.
(45) He, X.; Baumgartner, T. Conjugated Main-Group Polymers for Optoelectronics. *RSC Adv.* **2013**, *3*, 11334−11350.
(46) Xue, P.; Xu, Q.; Gong, P.; Qian, C.; Zhang, Z.; Jia, J.; Zhao, X.; Lu, R.; Ren, A.; Zhang, T. Two-Component Gel of a D−π−A−π−D Carbazole Donor and a Fullerene Acceptor. *RSC Adv.* **2013**, *3*, 26403−26411.
(47) Wang, X.; Liu, M. Vicinal Solvent Effect on Supramolecular Gelation: Alcohol Controlled Topochemical Reaction and the Toruloid Nanostructure. *Chem.—Eur. J.* **2014**, *20*, 10110−10116.
(48) Frisch, M. J.; Trucks, G. W.; Schlegel, H. B.; Scuseria, G. E.; Robb, M. A.; Cheeseman, J. R.; Scalmani, G.; Barone, V.; Mennucci, B.; Petersson, G. A.; Nakatsuji, H.; Caricato, M.; Li, X.; Hratchian, H. P.; Izmaylov, A. F.; Bloino, J.; Zheng, G.; Sonnenberg, J. L.; Hada, M.; Ehara, M.; Toyota, K.; Fukuda, R.; Hasegawa, J.; Ishida, M.; Nakajima, T.; Honda, Y.; Kitao, O.; Nakai, H.; Vreven, T.; Montgomery, J. A., Jr.; Peralta, J. E.; Ogliaro, F.; Bearpark, M.; Heyd, J. J.; Brothers, E.; Kudin, K. N.; Staroverov, V. N.; Kobayashi, R.; Normand, J.; Raghavachari, K.; Rendell, A.; Burant, J. C.; Iyengar, S. S.; Tomasi, J.; Cossi, M.; Rega, N.; Millam, M. J.; Klene, M.; Knox, J. E.; Cross, J. B.; Bakken, V.; Adamo, C.; Jaramillo, J.; Gomperts, R.; Stratmann, R. E.; Yazyev, O.; Austin, A. J.; Cammi, R.; Pomelli, C.; Ochterski, J. W.; Martin, R. L.; Morokuma, K.; Zakrzewski, V. G.; Voth, G. A.; Salvador, P.; Dannenberg, J. J.; Dapprich, S.; Daniels, A. D.; Farkas, Ö.;

Foresman, J. B.; Ortiz, J. V.; Cioslowski, J.; Fox, D. J. *Gaussian 09w*, Revision A.02, Gaussian, Inc.: Wallingford, CT, 2009.
(49) Rahman, M. M.; Czaun, M.; Takafuji, M.; Ihara, H. Synthesis, Self-Assembling Properties, and Atom Transfer Radical Polymerization of an Alkylated L-Phenylalanine-Derived Monomeric Organogel from Silica: A New Approach to Prepare Packing Materials for High-Performance Liquid Chromatography. *Chem.—Eur. J.* **2008**, *14*, 1312−1321.
(50) Karsten, B. P.; Bijleveld, J. C.; Viani, L.; Cornil, J.; Gierschner, J.; Janssen, R. A. J. Electronic Structure of Small Band Gap Oligomers Based on Cyclopentadithiophenes and Acceptor Units. *J. Mater. Chem.* **2009**, *19*, 5343−5350.
(51) Grisorio, R.; Dell'Aquila, A.; Romanazzi, G.; Suranna, G. P.; Mastrorilli, P.; Cosma, P.; Acierno, D.; Amendola, E.; Ciccarella, G.; Nobile, C. F. Novel Bifluorene Based Conjugated Systems: Synthesis and Properties. *Tetrahedron* **2006**, *62*, 627−634.
(52) Bao, C.; Lu, R.; Jin, M.; Xue, P.; Tan, C.; Liu, G.; Zhao, Y. L-Tartaric Acid Assisted Binary Organogel System: Strongly Enhanced Fluorescence Induced by Supramolecular Assembly. *Org. Biomol. Chem.* **2005**, *3*, 2508−2512.
(53) Jia, J.; Zhang, Y.; Xue, P.; Zhang, P.; Zhao, X.; Liu, B.; Lu, R. Synthesis of Dendritic Triphenylamine Derivatives for Dye-Sensitized Solar Cells. *Dyes Pigments* **2013**, *96*, 407−413.
(54) Lim, K.; Ju, M. J.; Na, J.; Choi, H.; Song, M. Y.; Kim, B.; Song, K.; Yu, J.; Kim, E.; Ko. Molecular Engineering of Organic Sensitizers with Planar Bridging Units for Efficient Dye-Sensitized Solar Cells. *J. Chem. Eur. J.* **2013**, *19*, 9442−9446.
(55) Jintoku, H.; Yamaguchi, M.; Takafuji, M.; Ihara, H. Molecular Gelation-Induced Functional Phase Separation in Polymer Film for Energy Transfer Spectral Conversion. *Adv. Funct. Mater.* **2014**, *24*, 4105−4112.
(56) Zhou, J.; Zuo, Y.; Wan, X.; Long, G.; Zhang, Q.; Ni, W.; Liu, Y.; Li, Z.; He, G.; Li, C.; Kan, B.; Li, M.; Chen, Y. Solution-Processed and High-Performance Organic Solar Cells Using Small Molecules with a Benzodithiophene Unit. *J. Am. Chem. Soc.* **2013**, *135*, 8484−8487.
(57) Xue, P.; Chen, P.; Jia, J.; Xu, Q.; Sun, J.; Yao, B.; Zhang, Z.; Lu, R. A Triphenylamine-Based Benzoxazole Derivative as a High-Contrast Piezofluorochromic Material Induced by Protonation. *Chem. Commun.* **2014**, *50*, 2569−2571.
(58) Xue, P.; Lu, R.; Yang, X.; Zhao, L.; Xu, D.; Liu, Y.; Zhang, H.; Nomoto, H.; Takafuji, M.; Ihara, H. Self-Assembly of a Chiral Lipid Gelator Controlled by Solvent and Speed of Gelation. *Chem.—Eur. J.* **2009**, *15*, 9824−9835.
(59) Jintoku, H.; Takafuji, M.; Oda, R.; Ihara, H. Enantioselective Recognition by a Highly Ordered Porphyrin-Assembly on a Chiral Molecular Gel. *Chem. Commun.* **2012**, *48*, 4881−4883.
(60) Wu, H.; Xue, L.; Shi, Y.; Chen, Y.; Li, X. Organogels Based on J- and H-Type Aggregates of Amphiphilic Perylenetetracarboxylic Diimides. *Langmuir* **2011**, *27*, 3074−3082.
(61) Xue, P.; Lu, R.; Chen, G.; Zhang, H.; Nomoto, H.; Takafuji, M.; Ihara, H. Functional Organogel Based on a Salicylideneaniline Derivative with Enhanced Fluorescence Emission and Photochromism. *Chem.—Eur. J.* **2007**, *13*, 8231−8239.
(62) Beckers, E. H. A.; Chen, Z.; Meskers, S. C. J.; Jonkheijm, P.; Schenning, A. P. H. J.; Li, X.; Osswald, P.; Würthner, F.; Jannssen, R. A. J. The Importance of Nanoscopic Ordering on the Kinetics of Photoinduced Charge Transfer in Aggregated π-Conjugated Hydrogen-Bonded Donor−Acceptor Systems. *J. Phys. Chem. B* **2006**, *110*, 16967−16979.
(63) Gellman, S. H.; Dado, G. P.; Liang, G. B.; Adams, B. R. Conformation-Directing Effects of a Single Intramolecular Amide−Amide Hydrogen Bond: Variable-Temperature NMR and IR Studies on a Homologous Diamide Series. *J. Am. Chem. Soc.* **1991**, *113*, 1164−1173.
(64) Dumur, F.; Contal, E.; Wantz, G.; Phan, T. N. T.; Bertin, D.; Gigmes, D. Immobilization of Styrene-Substituted 1,3,4-Oxadiazoles into Thermoreversible Luminescent Organogels and Their Unexpected Photocatalyzed Rearrangement. *Chem.—Eur. J.* **2013**, *19*, 1373−1384.
(65) Wu, Y.; Hirai, Y.; Tsunobuchi, Y.; Tokoro, H.; Eimura, H.; Yoshio, M.; Ohkoshi, S.; Kato, T. Supramolecular Approach to the Formation of Magneto-Active Physical Gels. *Chem. Sci.* **2012**, *3*, 3007−3010.
(66) Rao, M. R.; Sun, S. Supramolecular Assemblies of Amide-Derived Organogels Featuring Rigid π-Conjugated Phenylethynyl Frameworks. *Langmuir* **2013**, *29*, 15146−15158.
(67) Pan, S.; Luo, S.; Li, S.; Lai, Y.; Geng, Y.; He, B.; Gu, Z. Ultrasound Accelerated Gelation of Novel L-Lysine Based Hydrogelators. *Chem. Commun.* **2013**, *49*, 8045−8047.
(68) Zhang, T.; Lu, R.; Zhang, H.; Xue, P.; Feng, W.; Liu, X.; Zhao, B.; Zhao, Y.; Li, T.; Yao, J. Highly Ordered Photoluminescent Self-assembled Films Based on Polyoxotungstoeuropate Complex $Na_9[EuW_{10}O_{36}]$. *J. Mater. Chem.* **2003**, *13*, 580−584.
(69) Wood, J. D.; Jellison, J. L.; Finke, A. D.; Wang, L.; Plunkett, K. N. Electron Acceptors Based on Functionalizable Cyclopenta[hi]-aceanthrylenes and Dicyclopenta[de,mn]tetracenes. *J. Am. Chem. Soc.* **2012**, *134*, 15783−15789.
(70) Nakanishi, T.; Kojima, T.; Ohkubo, K.; Hasobe, T.; Nakayama, K.; Fukuzumi, S. Photoconductivity of Porphyrin Nanochannels Composed of Diprotonated Porphyrin Dications with Saddle Distortion and Electron Donors. *Chem. Mater.* **2008**, *20*, 7492−7500.